Growth and Virulence Alterations of Equine Herpesvirus 1 by Insertion of a Green Fluorescent Protein Gene in the Intergenic Region between ORFs 62 and 63

El Sayed Moustafa Ibrahim[1], Ochir Pagmajav[1], Tsuyoshi Yamaguchi[1,2], Tomio Matsumura[3], and Hideto Fukushi*[,1,2]

[1]*Department of Applied Veterinary Sciences, United Graduate School of Veterinary Sciences,* [2]*Laboratory of Veterinary Microbiology, Faculty of Applied Biological Sciences, Gifu University, Gifu, Gifu 501–1193, Japan, and* [3]*Epizootic Research Station, Equine Research Institute, The Japanese Racing Association, Tochigi 329–0412, Japan*

Abstract: **Nucleotide sequences of the intergenic region between ORF 62 and ORF 63 of equine herpesvirus 1 (EHV-1) isolates were analyzed. The sequences of this region consisted of variable and conserved domains among EHV-1 isolates. An EHV-1 mutant, Ab4-GFP, was constructed by inserting a green fluorescent protein (GFP) expression cassette flanked by *lox*P at both ends into the intergenic region between ORF 62 and ORF 63. Another mutant, Ab4-loxP, which contains one *lox*P site, was constructed by excision of the GFP cassette from the Ab4-GFP virus genome by cre enzyme. The recombinant Ab4-GFP formed smaller plaques than the wild type in MDBK cells. Virus production also decreased for Ab4-GFP in multistep growth analyses. Virulence of Ab4-GFP in both mice and hamsters was weaker than that of the wild type. Ab4-loxP exhibited properties similar to those of the wild type. These results suggest that the intergenic region between ORF 62 and ORF 63 plays various roles in the virus growth.**

Key words: **EHV-1, GFP, Intergenic region, Pathogenicity**

Equine herpesvirus 1 (EHV-1) is endemic in horse populations throughout the world, causing respiratory infections, epizootic abortion and neurological disorders in horses (2, 6, 14). The economic impact of EHV-1 infections is large in the horse industry. However, the molecular mechanism of EHV-1 pathogenicity is unclear.

The EHV-1 genome is composed of a unique long (U_L) region and a unique short (U_S) region which is flanked by two inverted repeat regions (IR_S and TR_S) and encodes at least 72 unique genes and at least 4 diploid genes (11, 19, 20).

The EHV-1 genome contains five sizeable regions appearing not to encode proteins. The first is approximately 1 kbp in size and is located at the left end of the viral genome (19). The second is approximately 1 kbp in size and is located between ORF 39 and ORF 40.

The third is approximately 1.5 kbp in size and is located between ORF 62 and ORF 63. The fourth, approximately 2 kbp in size, is located between ORF 63 and ORF 64 in the U_L/IR_S junction. The fifth region is a 2.5 kbp non-coding region that is located between ORF 64 and ORF 65 in IR_S and TR_S.

The functions of the intergenic regions have been speculated, based on their nucleotide sequences. The non-coding region at the left end of the genome in U_L may be involved in genomic cleavage in the replication of viral genome DNA (5, 21). The non-coding region between ORF 39 and ORF 40 contains the replication origin, ori_L (15). The non-coding region between ORF

---

*Address correspondence to Dr. Hideto Fukushi, Laboratory of Veterinary Microbiology, Faculty of Applied Biological Sciences, Gifu University, 1–1 Yanagido, Gifu, Gifu 501–1193, Japan. Fax: +81–58–293–2946. E-mail: hfukushi@cc.gifu-u.ac.jp

64 and ORF 65 in IR$_S$ and TR$_S$ contains a replication origin, ori$_S$ (3, 19). Csellner et al. (7) reported that insertion of a *lac*Z cassette in the second region between ORF 62 and ORF 63 without any deletion of viral genome sequences did not interfere with the expression of the flanking genes and the resulting mutant exhibited growth properties similar to those of the parent EHV-1. There is no report about the function of the non-coding region between ORF 63 and ORF 64.

Many methods have been used for targeting DNA recombination. The cre/*lox*P recombination system using a cre recombinase and *lox*P sites is known to be useful for excising a DNA fragment with the *lox*P sequence at the edges under the control of the cre recombinase expression (1, 18), though a *lox*P sequence remains at the site after excision.

In this study, we compared nucleotide sequences of the intergenic region between ORF 62 and ORF 63 among field isolates of EHV-1. We constructed recombinant viruses of EHV-1 Ab4p by insertion of a green fluorescent protein (GFP) expression cassette with *lox*P sequences and excision of the cassette by a cre recombinase in this region without deletion of any viral genomic sequences. We then analyzed the virological properties of the recombinant viruses in cell culture and in both mice and hamster experimental infection models. The nucleotide sequences of this region consisted of variable and conserved domains. The GFP-inserted recombinant virus (Ab4-GFP) had lower virulence and growth in cell culture than the wild type, although the properties of a recombinant with only the *lox*P sequence were identical to those of the parent Ab4p. These results indicate that the intergenic region between ORF 62 and ORF 63 might have a certain function in the virus growth.

Materials and Methods

Viruses and cells. EHV-1 Ab4p was kindly provided by Dr. A.J. Davison, Glasgow University, Scotland. Six field EHV-1s were isolated in different outbreaks among horses in Japan (Table 1). These isolates had different passage histories in cell culture.

Viruses were propagated in fetal horse kidney (FHK) cells. Virus titration, plaque assay and plaque purification were examined in Madin-Darby bovine kidney (MDBK) cells. FHK and MDBK cells were grown in Eagle's minimum essential medium (Eagle's MEM) (Nissui, Japan) supplemented with 100 IU/ml penicillin, 100 μg/ml streptomycin and 5% fetal bovine serum (FBS).

Virus titration. Virus titers were determined by plaque assay in MDBK cells. Briefly, 10-fold dilutions of the virus were adsorbed onto MDBK cells. After 90 min of adsorption at 37 C in 5% CO$_2$, the inoculum was removed and fresh medium containing 1.5% carboxymethylcellulose was added. After 3 days incubation at 37 C in 5% CO$_2$, cells were stained with crystal violet solution (20 g/liter crystal violet, 50% methanol, 20% acetic acid, 25% formalin).

DNA extraction. Total DNA was extracted from virus-infected FHK cells as described previously (10).

DNA sequencing. Four sets of PCR primers were designed for the sequencing (Table 2). DNA was amplified with an initial denaturation step at 94 C for 4 min, followed by 30 cycles consisting of 94 C denaturation for 30 sec, 60 C annealing for 20 sec and 72 C extension for 1 min. The four overlapped PCR fragments were cloned into the pGEM Easy T-vector (Promega, Japan) separately. Sequencing was done with M13-47 forward and RV-M reverse primers. Sequences were analyzed using GENETYX-MAC ver. 12 software. Sequence alignments were performed using CLUSTAL X (12). The phylogenic tree was constructed by the neighborhood-joining method (16) using PHYLIP software (10).

Construction of the recombinant plasmids. A 550-bp PCR fragment corresponding to the nucleotides 109767 to 110317 of the Ab4p genome containing the insertion point was amplified by PCR using Ex-*Taq* polymerase (TaKaRa, Japan). The PCR product was ligated with the pUC19 (Amersham Pharmacia Biotech, Japan) at the *Sma*I site (Fig. 1). The resulting plasmid was designated as pE1. A GFP expression cassette 1,640-bp frag-

Table 1. EHV-1 strains which were used in this study

Strain	Source	Pathogenicity in hamster*	Country	Reference
Ab4p	Abortion. Respiratory system	Severe	U.K.	Telford et al. (19)
89c104	Nasal swab. Respiratory system	Severe	Japan	Matsumura et al. (unpublished)
89c103	Nasal swab. Respiratory system	Low virulent	Japan	Matsumura et al. (unpublished)
90c16	Nasal swab. Respiratory system	Non virulent	Japan	Matsumura et al. (unpublished)
97c5	Embryo lung. Abortion	Non virulent	Japan	Matsumura et al. (unpublished)
97c9	Embryo lung. Abortion	Non virulent	Japan	Matsumura et al. (unpublished)
98c16	Embryo lung. Abortion	Non virulent	Japan	Matsumura et al. (unpublished)

* Manuscript in preparation.

Table 2. Nucleotide sequences of primers for PCR and sequencing

Primer	Sequence	Location in Ab4p
Sen F	5' GGG CTT TTG TGG TAT ATA GGT ATG CAC GCG GTG GAC 3'	109767–109802
Anti R	5' CTA TCA GTC TGA GAG AGT GTT AAT AGT CGC CGC CC 3' NheI AflII	110317–110282
Sens-loxP	5' GGG CTA GCT TAA GAT AAC TTA GTA TAA TGT ATG CTA TAC GAA GTT ATC GAT GCT GTA ATC GCC TTA 3' NheI NsiI	110055–110034
Anti-loxP	5' GGG CTA GCA TGC ATA TAA CTT CGT ATA GCA TAC ATT ATA CGA AGT TAT TGT TTC AAG GCG GTG TTT GGG A 3'	110056–110077
Sens 62–63	5' CCA ATC CCT GAA CGA CTG CAA ACG GAT TAA CCC AAA CCG G 3'	08382–108421
Anti 62–63	5' GGC CAA ACC CTT AAC TAT GCA ACC CCA AAA AGC AGC GTA G 3'	112321–112282
FC2*	5' CTT GTG AGA TCT AAC CGC AC 3'	1477–1496
R1*	5' GCG TTA TAG CTA TCA CGT CC 3'	1936–1917
SF1	5' CCG GTC GTT CGG TTG AGC AAG TTT TTG ATG 3'	108486–108515
SR1	5' CCT CCA GTC CAC AGA TAT GAC ATC CAA AGG 3'	109141–109112
SF2	5' ACC GGA AGC TTG TCA TAT TTG TGA GCC TGG 3'	109042–109071
SR2	5' TGT GAA CAT CAC CAC CAA TAC CAA GCA CGG 3'	109734–109705
SF3	5' CC AAT TAG CCC CCA ATT GGC ACA TGG TAA 3'	109660–109689
SR3	5' TTA CAA AAA CCT ATG CAG GGG TGT GGG TGG 3'	110265–110236
SF4	5' TTC CCC CGG GCC TTA TAT CTT GCA GCT TTA 3'	110104–110134
SR4	5' TTG TTT TAG TCG ACC GAA GCT CTG AGG GAG 3'	110681–110652
RNA-F1	5' ATG AGG GTC AGA GGT TAG ATC CAA GCA ACC 3'	108891–108920
RNA-R1	5' TGG TGG GAA TAT TAC AGC TTC CTG GGC GTT 3'	109198–109169
RNA-F2	5' CCG TGC TTG GTA TGG GTG GTG ATG TTC ACA 3'	109705–109734
RNA-R2	5' GAA GAC CCC CAA GCG TTT ACC TAT TCC ATG 3'	109991–109962
RNA-F3	5' GGC GAT TAT TAC AGC ATC GTG TTT CAA GGC GC 3'	110037–110068
RNA-R3	5' TCA GTC TGA GAG AGT GTT AAT AGT CGC CGC 3'	110314–110285
RNA-F4	5' GGT CCC CAT GTG AAA TCT AGC CTT GTT GCT 3'	108594–108623
RNA-R4	5' GGT TGC TTG GAT CTA ACC TCT GAC CCT CAT 3'	108920–108891
RNA-F5	5' GAT AAG CAC TGG CTG ATC GGT GGT ATT CAG 3'	110971–111000
RNA-R5	5' GAA GAT ACG AGC GAT GAA ACC AGC ACA GAC 3'	111279–111250

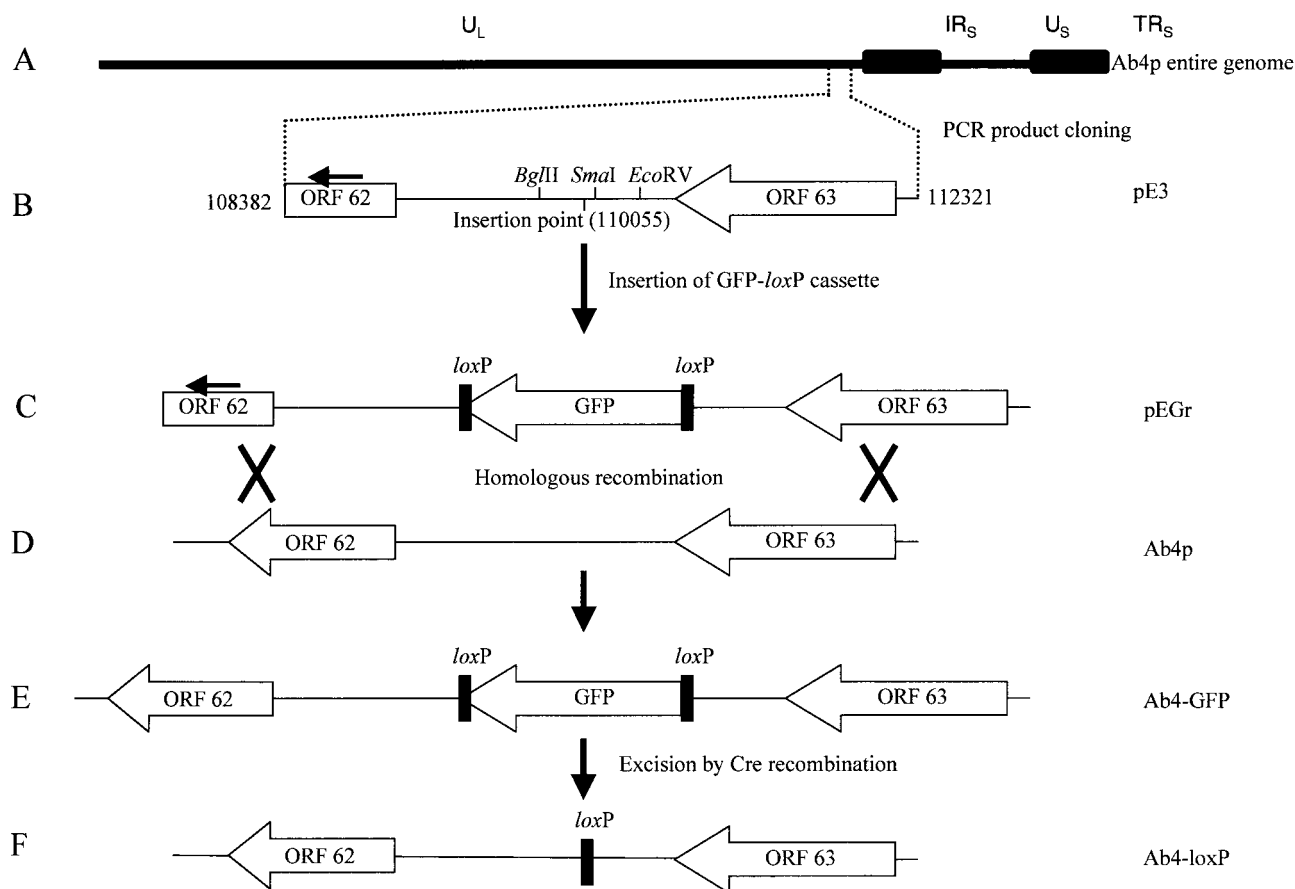* Primer designed by Kirisawa et al. (13).

Fig. 1. Scheme of the construction of the recombinant viruses. (A) Diagram of the EHV-1 genome. (B) We amplified a fragment corresponding to the nucleotides 108382 to 112321 of the Ab4p genome by PCR. The PCR product was cloned into the pT7-T vector to construct the pE3 plasmid. (C) GFP cassette was inserted into pE3 plasmid to construct the recombinant plasmid (pEGr). The insertion point was between the nucleotides 110055 and 110056 of the Ab4p genome. (D) MDBK cells were infected with Ab4p and transfected with pEGr to construct the recombinant Ab4-GFP by homologous recombination. (E) The recombinant Ab4-GFP contains the GFP-expression cassette flanked by two *lox*P sites. (F) The recombinant Ab4-loxP was constructed by excision of the GFP cassette by cre recombination in MDBK cells. Abbreviations: IR and TR, internal and terminal repeat sequences, respectively; U_L, unique long region; U_S, unique short region.

ment from the pEGFP-N1 (Clontech, U.S.A.) representing the GFP expression cassette containing the CMV/IE promoter and flanked by two *lox*P sites was inserted downstream of ORF 63 as follows. Two PCR primers (Sens-loxP and Anti-loxP) were designed to contain a *lox*P site and restriction sites as shown in Table 2. Each primer was used in a separate PCR that resulted in amplification of the 550-bp fragment. Both fragments were cut internally with *Bgl*II (the sense *lox*P fragment), *Eco*RV (the antisense *lox*P fragment), and *Nhe*I (both). Simultaneously, pE1 was digested with both *Bgl*II and *Eco*RV. Both the sense *lox*P and antisense *lox*P fragments were ligated with each other at *Nhe*I site and with pE1 in *Bgl*II and *Eco*RV sites through a triple ligation. The resulting clone, designated as pE2, contained an *Nsi*I and an *Afl*II site flanked by two *lox*P sites in the same orientation with each other (Fig. 1). A

1,640-bp fragment from the pEGFP-N1 representing the GFP expression cassette was inserted into the *Nsi*I and *Afl*II sites resulting in the pEG1 plasmid.

A 3,939-bp PCR fragment, corresponding to the nucleotides 108382 to 112321 of the Ab4p genome, containing ORF 62 and downstream of ORF 63 was cloned into the pT7Blue vector (Novagen, Japan). The resulting clone was designated as pE3. The recombinant plasmid, pEGr, was constructed by cloning the GFP cassette flanked by two *lox*P sites (from pEG1 plasmid) into the *Bgl*II and *Eco*RV sites of the pE3 plasmid (Table 2 and Fig. 1).

Homologous recombination. A monolayer of MDBK cells in a 6-well plate was infected by Ab4p at an MOI of 0.4. After 90 min of adsorption, cells were transfected by 4 μg/well of pEGr plasmid (Fig. 1) which was linearized by digestion with *Spe*I by using 10 μl/well of

Lipofectamine 2000 (Invitrogen, Japan). When 90% of the cells showed CPE, the supernatant was collected.

Appropriate dilutions of the virus stock were inoculated into MDBK cells. After 90 min of adsorption, cells were covered by fresh MEM containing 5% of FBS and 1.5% of carboxymethylcellulose, and incubated for 3 days at 37 C. The desired virus was identified and selected under fluorescent microscopy. Recombinant viruses were purified by three rounds of plaque purification. Recombinant viruses were verified by PCR. PCR assays were carried out to detect the presence of the GFP cassette and the *lox*P sequence in the genome of Ab4-GFP. Specific primers were used (Table 2) to identify the recombinant viruses with Ex-*Taq* polymerase. DNA amplification was performed with an initial denaturation step at 94 C for 4 min, followed by 30 cycles consisting of 95 C denaturation for 30 sec, 64 C annealing for 20 sec and 72 C extension for 2 min. The presence of the GFP cassette flanked by two *lox*P sites was confirmed by sequencing.

Cre recombination. To remove the GFP cassette from Ab4-GFP virus (Fig. 1), MDBK cells were inoculated with Ab4-GFP at an MOI of 0.4 and then transfected with 2 µg/well of pxCANCre plasmid (17) (obtained from Riken under the permission of Dr. Saito, Tokyo University) by using 10 µl/well of Lipofectamine 2000. When 90% of the cells showed CPE, the supernatant was collected. After three times plaque purification the desired non-fluorescent plaques were identified and selected under fluorescent microscopy. The presence of a *lox*P sequence was confirmed by sequencing.

Virus growth kinetics. Confluent monolayers of MDBK cells in 6-well plates were infected with the viruses at an MOI of 1. After 90 min adsorption at 37 C, cells were rinsed for 1 min with MEM to remove the unabsorbed viruses. Cells were then incubated with fresh MEM supplemented with 2% FBS. At 0, 8, 16, 24, 32, 40, 48, 60 and 72 hr post-infection, supernatant and infected cells were collected separately. The extracellular and intracellular virus titers were determined by plaque assay.

Plaque size measurements. The average sizes of plaques in MDBK cells were measured after 3 days post-inoculation. The diameters of 100 randomly selected plaques were measured by using NIH Image 1.63 soft-ware. Student's *t*-test was employed to compare the mean plaque sizes of the viruses examined.

RT-PCR. MDBK cells in 6-well plates were inoculated with either wild type or recombinant viruses. Cells were harvested at 6 hr and 24 hr post-inoculation. Total RNA was extracted using TRIZOL reagent (Invitrogen) and resuspended in 15 µl DEPC-treated distilled water. Total RNA was treated with RNase-free DNase I (TaKaRa) and incubated for 30 min at 37 C. Then RNA was extracted with phenol/chloroform (1:1) following standard procedures and resuspended into 15 µl DEPC-treated distilled water. Five microliters of RNA (250 ng) solution was heated at 95 C for 5 min for denaturation, combined with reverse transcriptase master mix consisting of 2.5 µl of 5× RT buffer (TOYOBO, Japan), 2.5 µl dNTP (TaKaRa), 1 µg of pd (N)$_6$ random hexamer (Amersham Pharmacia Biotech), 20 U RNase inhibitor (TOYOBO) and 25 U reverse transcriptase (TOYOBO). The reaction mixture was incubated at 42 C for 30 min followed by incubation at 94 C for 5 min to stop the reaction. PCR assays were carried out using specific primers for ORF 62, specific primers for the intergenic region and specific primers for ORF 63 (Table 2). cDNA amplification was performed by 30 cycles consisting of 94 C denaturation for 30 sec, 62 C annealing for 30 sec and 72 C extension for 30 sec followed by final extension at 72 C for 5 min.

Experimental infection of animals. Five-week-old specific pathogen-free (SPF) female BALB/c mice (SLC, Japan) and 3-week-old SPF male Syrian hamsters (SLC) were used in this study. Food and water were freely available during the course of the experiment. The mice and hamsters were observed for 3 days before the experiment. Animals were anesthetized by 2.5 mg/head of ketamine hydrochloride (Sankyo, Japan). All experiments were conducted under the guidelines for animal experiments in Gifu University with certification by the committee of Faculty of Applied Biological Sciences, Gifu University.

Mice were inoculated intranasally with 1×10^7 pfu/50 µl of MEM per animal. Body weight and clinical signs were monitored twice a day. Mice inoculated with viruses were euthanized by using an intraperitoneal injection of an excess amount of sodium pentobarbital. For virus isolation and DNA detection, lungs, spleen, liver and brain of two mice from each group were used. Tissues were homogenized in MEM at 10% (w/v). The homogenate was centrifuged at 3,000 rpm for 10 min to remove the cellular debris. Supernatant was serially 10-fold diluted in MEM and inoculated onto a confluent MDBK monolayer in 24-well plates. Virus titers were determined by plaque assay. The limit of virus detection in the organ homogenates was 2×10^2 pfu per gram of mice organs.

For virus DNA detection in mice organs, DNA was extracted with a Sepagene kit (Sanko Junyaku, Japan). DNA was detected by using primers for the glycoprotein B gene according to Kirisawa et al. (13).

Hamsters were divided into 9 groups (4 animals per group) and were intranasally inoculated with 50 µl (per

animal) containing different amounts of virus. Body weight and clinical signs were monitored twice a day. All animals were sacrificed at 15 days post-infection by injection of an excess amount of sodium pentobarbital. Blood samples were collected by heart puncture for serological examination.

Antibody was assayed by indirect fluorescent antibody technique as follows. MDBK cells were infected with viruses in 24-well microscope slides and incubated at 37 C for 10–12 hr. The fluid media was aspirated and the slides were dried for 10 min and then fixed with acetone for 10 min. Twenty-five microliters of twofold dilutions of hamster sera were added to the cells. The cells were incubated for 1 hr at 37 C and then washed

three times with PBS for 5 min. Twenty-five microliters of fluorescein-conjugated anti-hamster immunoglobulin G (IgG) monoclonal antibody (ICN Biomedicals, Inc., Japan) solution was placed on each well. Slides were incubated for 1 hr at 37 C, washed 3 times with PBS and once with distilled water, dried in air, and mounted in buffered glycerol. The antibody titration was determined under fluorescent microscopy.

Results

Nucleotide Sequence of the Intergenic Region between ORF 62 and ORF 63 in EHV-1 Isolates

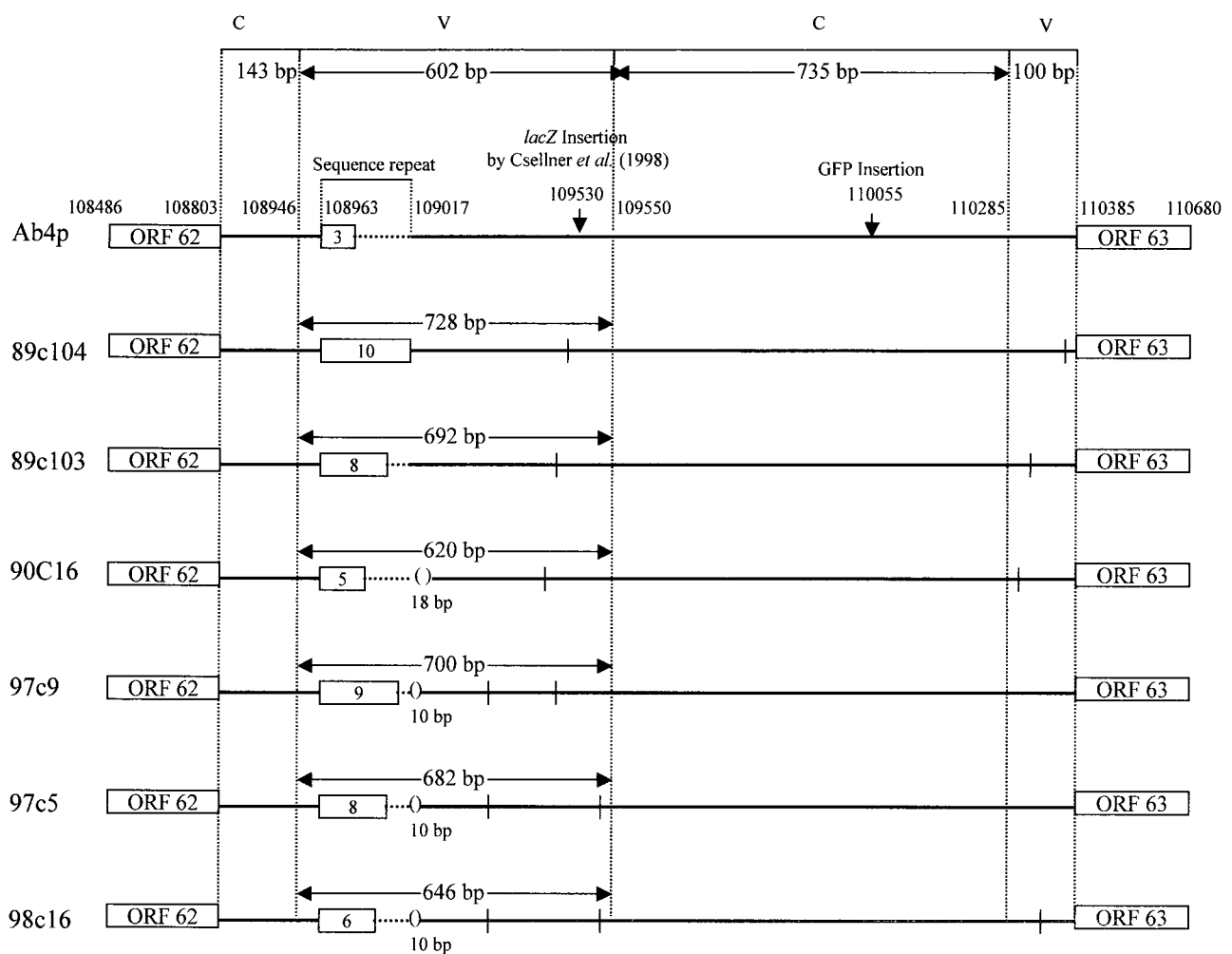The nucleotide sequence of the 2.2 kbp containing

Fig. 2. Multiple alignments of the nucleotide sequences of the non-coding region between ORF 62 and ORF 63. This region was divided into four domains. C: Two conserved domains among all EHV-1 isolates. The first conserved domain corresponded to the nucleotides 108803 to 108946 of the Ab4p genome. The second conserved domain corresponded to the nucleotides 109551 to 110285 of the Ab4p genome. V: Two variable domains which contain insertion, deletion mutations, in addition to base substitutions among the isolates. The first variable domain corresponded to the nucleotides 108947 to 109550 of the Ab4p genome. The second variable domain corresponded to the nucleotides 110286 to 110385 of the Ab4p genome. The variable domains contain insertion and deletion mutations. Insertion mutations are mainly 18-bp sequence repeats. The copy number of this repeat is different among the isolates. *lac*Z insertion by Csellner et al. (1998) was at the nucleotide 109530 of the HVS25A genome as indicated in the figure. □, 18-bp sequence repeat; |, base substitution; ( ), deletion.

the intergenic region between ORF 62 and ORF 63 of six EHV-1 field isolates showed four domains in this region. The first domain corresponding to nucleotide numbers 108803 to108945 in the Ab4p genome was conserved among all EHV-1 isolates examined (Fig. 2). The second domain corresponding to nucleotide numbers 108946 to 109550 in the Ab4p genome was variable among the isolates. This domain contained insertions and deletions compared to Ab4p. The insertion was mainly 18-bp sequence repeats. The number of the repeats was variable among the isolates (Fig. 2). The third domain corresponding to nucleotide numbers 109551 to 110286 in the Ab4p genome was conserved. The fourth domain corresponding to nucleotide numbers 110287 to 110385 in the Ab4p genome was variable. The variable regions showed base variation among the isolates (Fig. 2).

Construction of Recombinant Viruses

The GFP expression cassette flanked by two *lox*P sequences was inserted into the large intergenic region

in the viral genome (Fig. 1) in order to determine the roles of this region in the virus life cycle. The targeted insertion site was inside the 1,584-bp intergenic space located between ORF 62 and ORF 63, specifically between nucleotides 110055 and 110056 of the Ab4p genome (Fig. 1). EHV-1 Ab4p was inoculated into MDBK cells. The infected MDBK cells were transfected with the recombinant plasmid (pEGr) where the homologous recombination occurred. After three rounds of selection and plaque purification, one recombinant virus was cloned and designated Ab4-GFP. A *lox*P-containing mutant was also constructed by excision of the GFP expression cassette from the viral genome using cre recombination. The cloned virus without the GFP was designated as Ab4-loxP.

In Vitro Growth Kinetics of the Recombinant Viruses

Growth kinetics and plaque sizes of Ab4-GFP and Ab4-loxP were compared to those of Ab4p in MDBK cells in order to determine whether the insertion of GFP and the presence of a *lox*P sequence in the intergenic
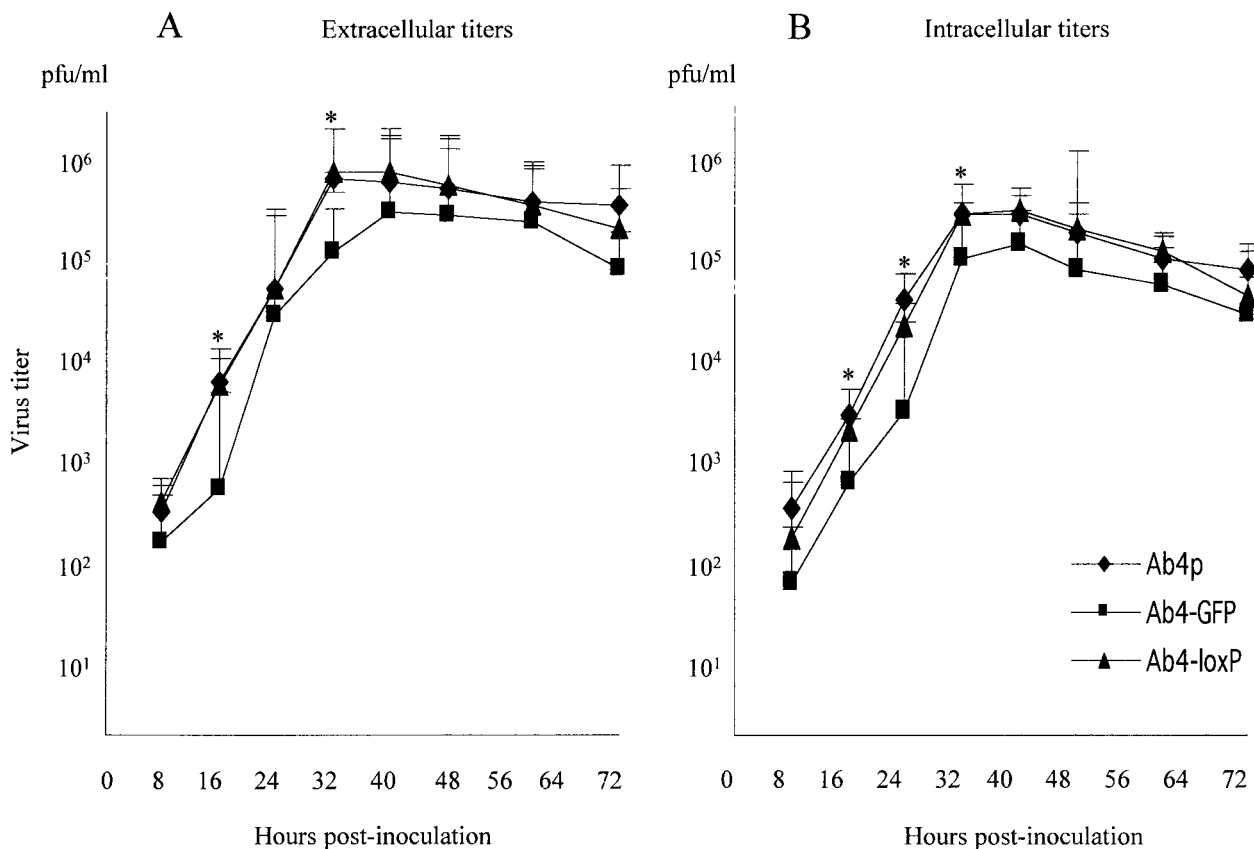

Fig. 3. Multi-step growth kinetics of Ab4p, Ab4-GFP and Ab4-loxP in MDBK cells. Kinetics of virus growth is depicted as virus titer determined in the extracellular (A) and intracellular (B) solutions. MDBK cells were infected with the various viruses at an MOI of 1 for 90 min at 37 C. Infected cells were washed and incubated with fresh medium. At the indicated times after infection, extracellular and intracellular virus titers were determined by titration on MDBK cells and are expressed as plaque-forming units (pfu). The extracellular and intracellular virus titers of Ab4-GFP were significantly lower than those of Ab4p and Ab4-loxP. The experiment was repeated 3 times. *$P<0.05$.

region between ORF 62 and ORF 63 had any effect on viral growth *in vitro*. In multi-step growth kinetics, the growth patterns of Ab4p and Ab4-loxP were similar. The extracellular and intracellular virus titers of Ab4p and Ab4-loxP reached their peak values at 40 and 32 hr post-inoculation, respectively (Fig. 3). On the other hand, both the extracellular and intracellular titers of Ab4-GFP were lower than those of Ab4p and Ab4-loxP. The peak extracellular and intracellular titers of Ab4-GFP were observed at 40 hr post-inoculation (Fig. 3). The peak titer of Ab4-GFP was significantly ($P<0.05$) lower than those of Ab4p and Ab4-loxP.

The average ($n=100$) plaque size of Ab4-GFP (2.45 mm^2) was significantly smaller ($P<0.05$) than those of Ab4p (2.85 mm^2) and Ab4-loxP (2.90 mm^2) in MDBK cells 3 days post-inoculation (Fig. 4).

RNA transcripts were investigated using specific primers, RNA-F1, RNA-R1, RNA-F2, RNA-R2, RNA-F3 and RNA-R3, for the intergenic region of recombinants and wild-type virus. No transcript for this region was detected in infected MDBK cells. The transcripts of ORF 62 and ORF 63 were detected by RT-PCR using specific primers, RNA-F4, RNA-R4, RNA-F5 and RNA-R5. No difference was found in the transcription of these genes among recombinants and wild-type virus.

Virulence of the Recombinant Viruses in Animal Models

The pathogenicity and virulence of the recombinant viruses were analyzed in murine and hamster models. All mice that were inoculated with the viruses showed less activity, ruffled fur, hunched posture and increased respiration rates. These symptoms started from the 2nd day post-inoculation in whole groups of mice. Symptoms disappeared by the 4th day post-inoculation in the Ab4-GFP-inoculated group and by the 5th day in the Ab4p- and Ab4-loxP-inoculated groups. Body weight loss was observed in all groups from the 2nd day post-inoculation until the 5th day in the Ab4-GFP-inoculated group and from the 2nd day post-inoculation until the 7th day in the Ab4p- and Ab4-loxP-inoculated groups. The Ab4p- and Ab4-loxP-inoculated groups did not
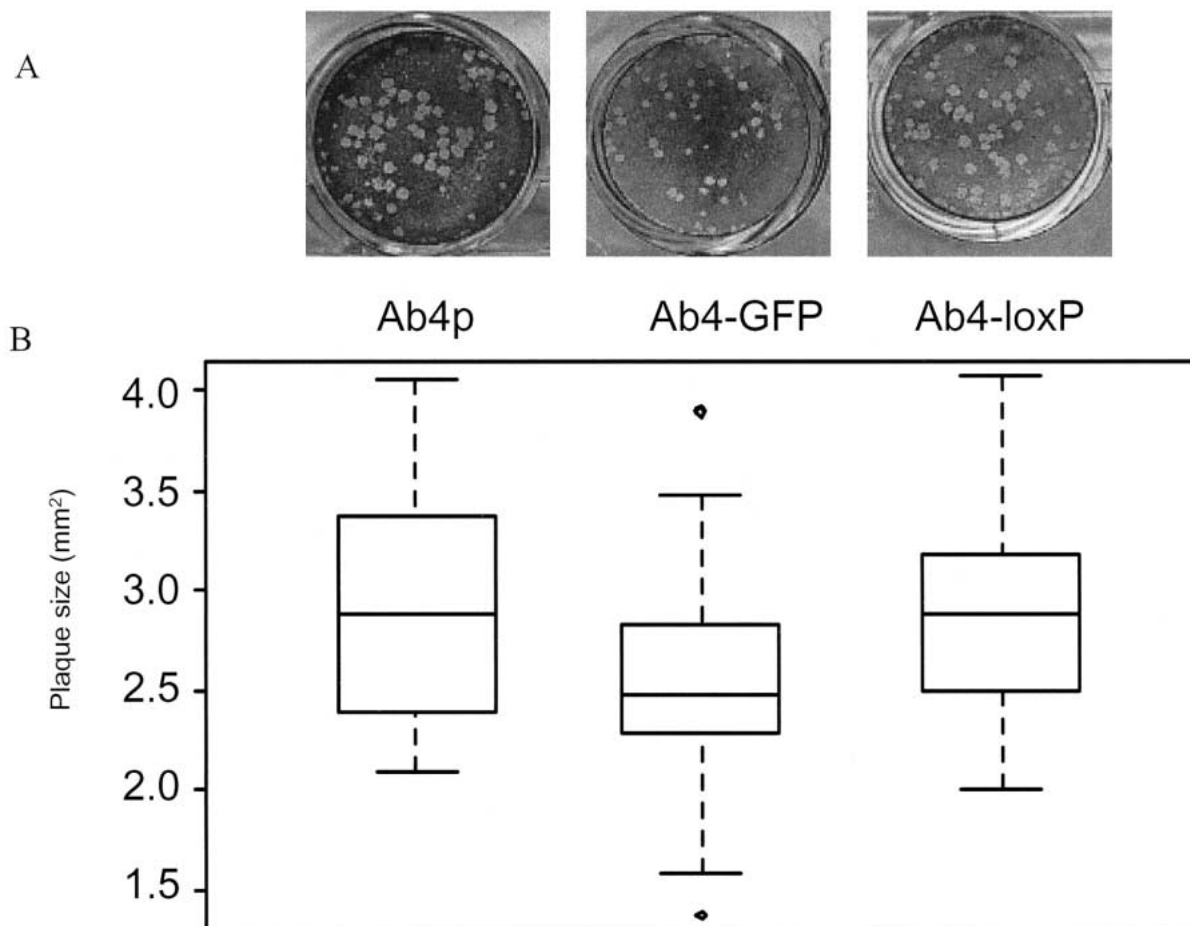

Fig. 4. Plaque size measurement of Ab4p, Ab4-GFP and Ab4-loxP. (A) The plaque size in MDBK cells at 3 days post-inoculation stained by crystal violet. (B) Average plaque sizes of 100 randomly selected plaques of the 3 viruses. The plaques formed by Ab4-GFP were significantly smaller than those formed by Ab4p and Ab4-loxP ($P<0.05$).

reach the pre-inoculation weight until the end of the observation period (Fig. 5).

Viruses were consistently recovered from lungs from the 1st day till the 6th day post-infection of mice inocu-

lated with Ab4p and Ab4-loxP. On the other hand, in the Ab4-GFP-inoculated mice, the virus was recovered from lungs from the 2nd day till the 4th day post-inoculation. Viruses were occasionally recovered from liver
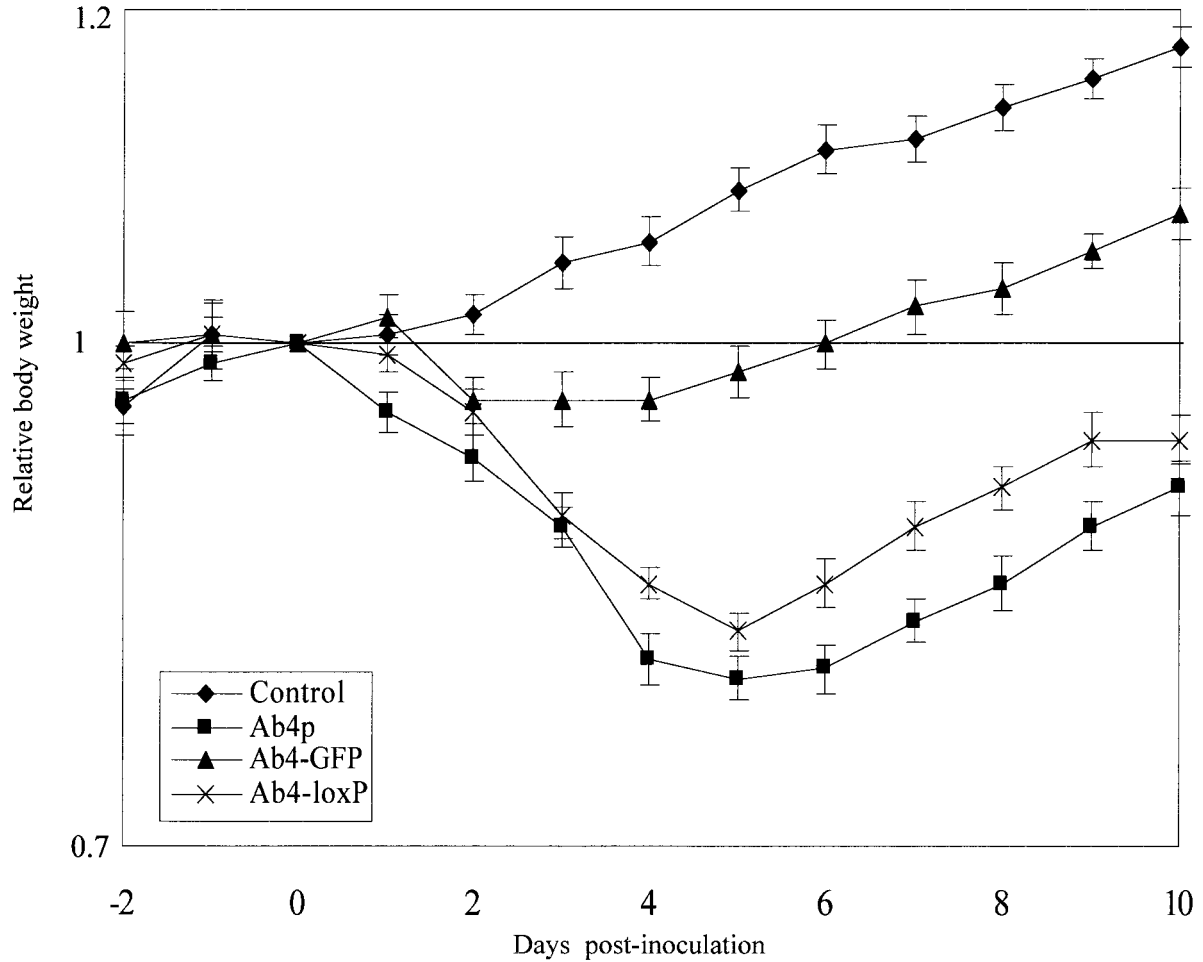

Fig. 5. Mice body weight gain after inoculation with Ab4p, Ab4-GFP and Ab4-loxP. Mice inoculated with Ab4p and Ab4-loxP experienced severe weight loss. Mice inoculated with Ab4-GFP experienced a transient weight loss.

Table 3. Virus titration and DNA detection in mice organs after inoculation of Ab4p, Ab4-GFP and Ab4-loxP

Virus	Organ	Days post-inoculation										
		0	1	2	3	4	5	6	7	8	9	10
Ab4p	Brain	$-/-$*	$-$**$/+$	$1\times10^4/+$	$6\times10^4/+$	$-/+$	$-/+$	$-/-$	$-/-$	$-/-$	$-/-$	$-/-$
	Lungs	$-/-$	$1\times10^4/+$	$6\times10^5/+$	$8\times10^8/+$	$1\times10^7/+$	$6\times10^4/+$	$1\times10^4/-$	$-/+$	$-/+$	$-/+$	$-/-$
	Liver	$-/-$	$2\times10^4/+$	$1\times10^5/+$	$-/+$	$-/-$	$-/-$	$-/-$	$-/-$	$-/-$	$-/-$	$-/-$
	Spleen	$-/-$	$-/+$	$-/+$	$-/-$	$-/-$	$-/-$	$-/-$	$-/-$	$-/-$	$-/-$	$-/-$
Ab4-GFP	Brain	$-/-$	$-/+$	$3\times10^4/+$	$-/+$	$-/+$	$-/-$	$-/-$	$-/-$	$-/-$	$-/-$	$-/-$
	Lungs	$-/-$	$-/+$	$2\times10^4/+$	$1\times10^7/+$	$1\times10^5/+$	$-/+$	$-/+$	$-/+$	$-/+$	$-/-$	$-/-$
	Liver	$-/-$	$-/+$	$1\times10^4/+$	$-/-$	$-/-$	$-/-$	$-/-$	$-/-$	$-/-$	$-/-$	$-/-$
	Spleen	$-/-$	$-/-$	$-/-$	$-/-$	$-/-$	$-/-$	$-/-$	$-/-$	$-/-$	$-/-$	$-/-$
Ab4-loxP	Brain	$-/-$	$-/+$	$1\times10^4/+$	$2\times10^5/+$	$-/+$	$-/+$	$-/-$	$-/-$	$-/-$	$-/-$	$-/-$
	Lungs	$-/-$	$1\times10^4/+$	$1\times10^5/+$	$6\times10^8/+$	$6\times10^6/+$	$2\times10^4/+$	$-/+$	$-/+$	$-/+$	$-/+$	$-/+$
	Liver	$-/-$	$2\times10^3/+$	$1\times10^5/+$	$-/+$	$-/-$	$-/-$	$-/-$	$-/-$	$-/-$	$-/-$	$-/-$
	Spleen	$-/-$	$-/+$	$-/+$	$-/-$	$-/-$	$-/-$	$-/-$	$-/-$	$-/-$	$-/-$	$-/-$

*: Virus titration/DNA detection. **: Titration less than 2×10^2 pfu/g of organ. $-$: Virus DNA was not detected. $+$: Virus DNA was detected.
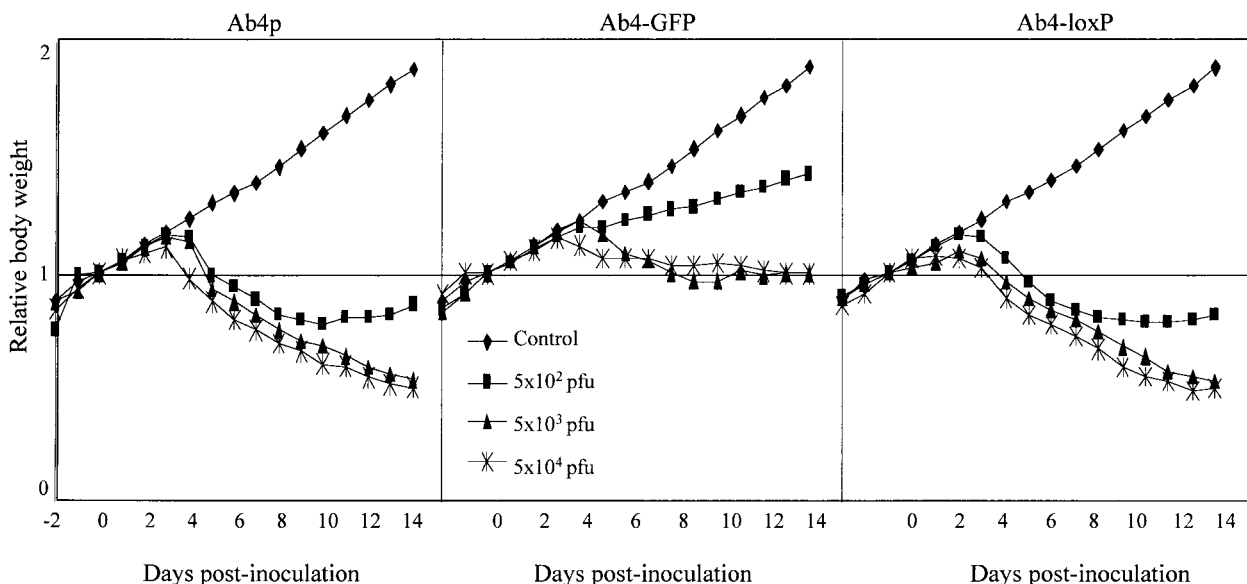
Fig. 6. Hamster body weight gain after intranasal inoculation of Ab4p, Ab4-GFP and Ab4-loxP. The weight loss of the Ab4-GFP-inoculated groups was mild and most animals regained their original weight before the end of the experiment.

Table 4. The nervous signs of hamsters after inoculation of Ab4p, Ab4-GFP and Ab4-loxP

Virus	Dose (pfu)	Days post-inoculation														
		0	1	2	3	4	5	6	7	8	9	10	11	12	13	14
	5×10^2	−	−	−	−	−	−	±	±	±	+	+	+	±	±	±
Ab4p	5×10^3	−	−	−	−	±	±	+	+	+	+	+	+	+	+	±
	5×10^4	−	−	−	±	+	+	+	+	+	+	+	+	+	+	+
	5×10^2	−	−	−	−	−	−	−	−	−	±	±	±	±	−	−
Ab4-GFP	5×10^3	−	−	−	−	−	−	±	±	±	+	+	+	±	±	±
	5×10^4	−	−	−	−	±	±	+	+	+	+	+	+	+	+	+
	5×10^2	−	−	−	−	−	±	±	±	+	+	+	+	±	±	±
Ab4-loxP	5×10^3	−	−	−	±	±	±	+	+	+	+	+	+	±	±	±
	5×10^4	−	−	−	±	+	+	+	+	+	+	+	+	+	+	+

−: No nervous signs. ±: Mild nervous signs. +: Severe nervous signs.

and brain of mice inoculated with Ab4p and Ab4-loxP from the 1st day till the 3rd day post-inoculation and only in the 2nd day post-inoculation in the Ab4-GFP-inoculated mice (Table 3). Virus DNA was detected in lungs of mice inoculated with Ab4p and Ab4-loxP from the 1st day post-inoculation till the 9th day, and from the 1st day till the 7th day post-inoculation in the Ab4-GFP-inoculated mice. No virus DNA was detected in the spleens of Ab4-GFP-inoculated mice (Table 3).

All hamsters inoculated with Ab4p and Ab4-loxP showed severe nervous manifestations, namely restlessness, incoordination and fighting with each other and aggressiveness, and finally lethargy which started from the 3rd day post-infection and persisted until the end of the experiment. Furthermore, severe weight loss was shown from the 3rd day of the experiment. Two Ab4p-infected hamsters and two Ab4-loxP-infected hamsters started to gain body weight at the 9th day post-infection.

In contrast, nervous signs were mild and started in two hamsters from the 4th day post-infection and then gradually appeared in all groups of hamsters inoculated with Ab4-GFP. The nervous signs disappeared in most of the hamsters before the end of the experiment. Furthermore, body weight loss was mild and started at the 4th and 5th days post-infection and most of the animals regained their body weight before the end of the experiment (Fig. 6 and Table 4). There was no significant difference in the antibody titers of the hamster sera.

Discussion

Sequence comparison revealed that the non-coding region between ORFs 62 and 63 consisted of conserved and variable domains. We inserted the GFP cassette at 1,254 bp upstream from the initiating codon of ORF 62 and 330 bp downstream from the termination of ORF 63

which is within a conserved region. The insertion mutant Ab4p-GFP formed smaller plaques and replicated less in MDBK cells than did Ab4p and Ab4-loxP. The virulence of the recombinant Ab4-GFP was also weaker in mice and hamsters. Construction of GFP-expressing viral mutants without any changes in the virus characters has been widely used (4, 8, 9). The present RT-PCR results showed that neither ORF 62 nor ORF 63 expression was affected by insertion of GFP. However, the insertion of the DNA fragment in the conserved domain reduced viral virulence. On the other hand, the virus containing only *lox*P exhibited the same virulence as the wild type. These results indicated that the length of the insert might be one of the factors that affect the virulence of the virus.

The variable domains contained 18-bp repeated sequences, base insertions and deletions, in addition to base variation among the isolates. The copy number of these repeats varied among the isolates. Csellner et al. (7) constructed a mutant virus by insertion of a *lac*Z gene at 720 bp upstream from the initiating codon for ORF 62 and 850 bp downstream from the termination of ORF 63 of the EHV-1 HVS25A strain, which corresponds to the variable domain. They concluded that the recombinant virus exhibited the same virulence as the wild type in mice. They also concluded that neither ORF 62 nor ORF 63 expression was affected by the insertion. Pagmajav et al. (manuscript in preparation) in our laboratory found one EHV-1 isolate from cattle that had a 0.8-kb deletion and a stretch of sequence repeats in the area where Csellner et al. (7) had inserted a *lac*Z fragment. These data suggest that this variable region is non-functional.

Our animal experiments in the present study revealed that Ab4-GFP had reduced virulence. The histopathological examinations showed that the pathological changes in the brain of the Ab4-GFP-inoculated mice were similar to those in the brain of the Ab4p-inoculated mice. However, the intensity of the lesions in the brain of the Ab4-GFP-inoculated mice was milder than that in the brain of the Ab4p-inoculated mice. Moreover, the number of antigen-positive neurons of the Ab4-GFP-inoculated mice was less than that of the Ab4p-inoculated mice (unpublished data). These results suggest that the reduced virulence of Ab4-GFP may be caused by less transmission to neurons or poor replication in neurons.

In conclusion, the conservation of the nucleotide sequences along with the alteration of virological properties of Ab4-GFP suggest that the non-coding region between ORF 62 and ORF 63 plays some roles in viral growth.

References

1) Adler, H., Messerle, M., Wagner, M., and Ulrich, H.K. 2000. Cloning and mutagenesis of the murine gammaherpesvirus 68 genome as an infectious bacterial artificial chromosome. J. Virol. **74**: 6964–6974.

2) Allen, G.P., and Bryans, J.T. 1986. Molecular epizootiology, pathogenesis, and prophylaxis of equine herpesvirus-1 infection. Prog. Vet. Microbiol. Immunol. **2**: 78–144.

3) Baumann, R.P., Ramana, V., Yalamanchili, R., and O'Callaghan, D.J. 1989. Functional mapping and DNA sequence of an equine herpesvirus 1 origin of replication. J. Virol. **63**: 1275–1283.

4) Breshears, M.A., Black, D.H., Ritchey, J.W., and Eberle, R. 2003. Construction and *in vivo* detection of an enhanced green fluorescent protein-expressing strain of Saimiriine herpesvirus 1 (SaHV-1). Arch. Virol. **148**: 311–327.

5) Chowdhury, S.I., Buhk, H.J., Ludwing, H., and Hammerscmidt, W. 1990. Genomic termini of equine herpesvirus type 1. J. Virol. **64**: 873–880.

6) Crabb, B.S., and Studdert, M.J. 1995. Equine herpesvirus 4 (equine rhinopneumonitis virus) and 1 (equine abortion virus). Adv. Virus Res. **45**: 153–190.

7) Csellner, H., Walker, C., Love, D.N., and Walley, J.M. 1998. An equine herpesvirus 1 mutant with a *lac*Z insertion between open reading frames 62 and 63 is replication competent and causes disease in the murine respiratory model. Arch. Virol. **143**: 2215–2231.

8) Demmin, G.L., Clase, A.C., Randall, J.A., Enquist, L.W., and Banfield, B.W. 2001. Insertions in the gG gene of pseudorabies virus reduce expression of the upstream Us3 protein and inhibit cell-to-cell spread of virus infection. J. Virol. **75**: 10856–10869.

9) Duprex, W.P., McQuaid, S., Roscic-Mrkic, B., Cattaneo, R., Mccallister, C., and Rima, B.K. 2000. *In vitro* and *in vivo* infection of neural cells by a recombinant measles virus expressing enhanced green fluorescent protein. J. Virol. **74**: 7972–7979.

10) Fukushi, H., Tomita, T., Taniguchi, A., Ochiai, Y., Kirisawa, R., Matsumura, T., Yanai, T., Masegi, T., Yamaguchi, T., and Hirai, K. 1997. Gazelle herpesvirus 1: a new neurotropic herpesvirus immunologically related to equine herpesvirus 1. Virology. **226**: 34–44.

11) Henry, B.E., Robinson, R.A., Dauenhauer, S.A., Atherton, S.S., Hayward, G., and O'Callaghan, D.J. 1981. Structure of the genome of equine herpesvirus type 1. Virology **115**: 97–114.

12) Jeannmougin, F., Thompson, J.D., Gouy, M., Higgins, D.G., and Gibson, T.J. 1998. Multiple sequence alignment with Clustal X. Trends Biochem. Sci. **23**: 403–405.

13) Kirisawa, H., Endo, A., Iwai, H., and Kawakami, Y. 1993. Detection and identification of equine herpesvirus-1 and-4 polymerase chain reaction. Vet. Microbiol. **36**: 57–67.

14) O'Callaghan, D.J., Genty, G.A., and Randall, C.C. 1983.

The equine herpesviruses, p. 215–318, vol. 2: comprehensive virology, Series 2, Plenum, New York.

15) Robertson, G.R., Scott, N.A., Miller, J.M., Sabine, M., Zheng, M., Bell, C.W., and Whalley, J.M. 1991. Sequence characteristics of a gene in equine herpesvirus 1 homologous to glycoprotein H of herpes simplex virus. DNA Sequence **1**: 241–249.

16) Saitou, N., and Nei, M. 1987. The neighbor-joining method: a new method for reconstructing phylogenetic trees. Mol. Biol. Evol. **4**: 406–425.

17) Sato, Y., Endo, H., Ajiki, T., Hakamata, Y., Okada, T., Murakami, T., and Kobayashi, E. 2004. Establishment of Cre/LoxP recombination system in transgenic rats. Biochem. Biophys. Res. Commun. **319**: 1197–1202.

18) Smith, G.A., and Enquist, L.W. 2000. A self-recombining bacterial artificial chromosome and its application for analysis of herpesvirus pathogenesis. Proc. Natl. Acad. Sci. U.S.A. **97**: 4873–4878.

19) Telford, E.A.R., Watson, M.S., McBride, K., and Davison, A.J. 1992. The DNA sequence of equine herpesvirus-1. Virology **189**: 304–316.

20) Whalley, J.M., Robertson, G.R., and Davison, A.J. 1981. Analysis of the genome of equine herpesvirus type 1: arrangement of cleavage sites for restriction endonucleases *Eco*RI, *Bgl*II and *Bam*HI. J. Gen. Virol. **57**: 307–323.

21) Yamanchili, R., and O'Callaghan, D.J. 1990. Sequence and organization of the genomic termini of equine herpesvirus type 1. Virus Res. **15**: 149–162.